Atmos. Chem. Phys. Discuss., 12, 22783–22811, 2012
www.atmos-chem-phys-discuss.net/12/22783/2012/
doi:10.5194/acpd-12-22783-2012

Atmospheric Chemistry and Physics Discussions

Meteorological observations in the Northern Chilean coast during VOCALS-REx

J. A. Rutllant[1,2], R. C. Muñoz[1], and R. D. Garreaud[1]

[1]Department of Geophysics, University of Chile, Santiago, Chile
[2]Centro de Estudios Avanzados en Zonas Aridas (CEAZA), La Serena, Chile

Received: 31 July 2012 – Accepted: 31 July 2012 – Published: 3 September 2012

Correspondence to: R. C. Muñoz (rmunoz@dgf.uchile.cl)

Published by Copernicus Publications on behalf of the European Geosciences Union.

Abstract

Surface coastal observations from two automatic weather stations at Paposo (∼25° S) and radiosonde observations at Paposo and Iquique (∼20° S), were carried out during VOCALS-REx. Within the coastal marine boundary layer (MBL), characteristic sea-land breezes are superimposed on the prevailing southerlies, resulting in light northeasterly winds from mid-night to early morning and strong near-surface southwesterlies in the afternoon. The prevailing northerly wind above the MBL and below the Andes top is modulated by the onshore–offshore (zonal) flow components induced by the diurnal cycle of net radiation along the western slope of the Andes. This diurnal cycle of the zonal regional circulation is consistent with an enhanced afternoon coastal subsidence manifested in a lower inversion base and a slight warming at its top. A numerical simulation of this zonal atmospheric circulation in a regional domain captures the afternoon zonal wind divergence and resulting subsidence along a narrow (∼10 km) coastal strip.

Day-to-day variability during VOCALS-REx shows subsynoptic oscillations in the MBL depth, aside from two major disruptions in connection with a deep trough and a cutoff low, as described elsewhere. These oscillations are phase-locked to those in sea-level pressure and afternoon alongshore southerlies, as found in connection with coastal lows farther south.

From a simple scale analysis, one can tentatively conclude that the mean offshore transport of sulfur dioxide from inner, elevated sources could be associated with the afternoon seaward flow with a delay of the order of at least one-day. Within the MBL, biogenic dimethylsulfide (DMS) could be more easily degassed in the afternoon due to the strengthening of the SW winds, while other coastal sources could contribute preferentially at dawn, coinciding with the maximum coastal low-cloud cover.

ACPD

12, 22783–22811, 2012

Meteorological observations during VOCALS-REx

J. A. Rutllant et al.

1 Introduction

The international VOCALS-Regional Experiment (VOCALS-REx) was aimed at studying interaction processes between ocean, atmosphere, cloud and land in the Southeastern Pacific, along and off the coasts of Southern Peru and Northern Chile (Wood et al., 2011). Over this region, dominated by the SE Pacific subtropical anticyclone with a marked subsidence temperature inversion at about 1000 m a.m.s.l., austral spring is the season of maximum intensity of the anticyclone featuring the most extensive and persistent stratocumulus (Sc) cloud deck topping the marine boundary layer (MBL) under the subsidence inversion (e.g. Painemal et al., 2010). It is well known that these clouds play a key role in the global radiation budget as well as in the regional climate along the coast (e.g. Bretherton et al., 2004).

A central aspect of VOCALS-REx was the quantitative assessment of the role of oxidized sulfur aerosols acting as Sc condensation nuclei in the near-shore region, particularly along Southern Peru and Northern Chile, producing high cloud droplet number concentrations (Wood et al., 2011). Natural sulfur emissions, that originate at the ocean surface, where coastal upwelling of nutrient-rich waters favors phytoplankton growth and subsequent dimethyl sulfide (DMS) emissions, become oxidized within the MBL (e.g. Spak et al., 2010). Also, several thermo-electric power plants along the coast and below the subsidence inversion contribute to these sulfur emissions as well. Inland over the Atacama desert and along the western slope of the Andes, at altitudes well above the MBL (i.e. 2–4 km), copper smelters and volcanoes farther inland make their contribution in terms of sulfur dioxide (Huneeus et al., 2006; Spak et al., 2010). Therefore, from a meteorological perspective, it becomes essential to understand the transport processes from the emission sources towards the cloud deck, both from within and above the MBL. This amounts first to characterizing the mean air flow and air temperature changes in the scales of hours (diurnal cycles) in the lower troposphere, basically controlled by the diurnal cycle of radiative warming/cooling over the coastal and Atacama deserts, and along the western slope of the Andes.

ACPD
12, 22783–22811, 2012

Advances towards understanding the basic features of the regional circulation across a zonal transect in Northern Chile at ~23° S were attempted during the DICLIMA experiment (Rutllant et al., 1998, 2003), in which strong diurnal cycles in temperature and winds were identified, spanning most of the troposphere below the Andes. Diurnal cycles in the winds above the subsidence inversion alternate from daytime eastward (inland) flow to nighttime westward flow in the lower layers with corresponding return flows aloft. Assuming mean uniform winds from the NW above the MBL over the coast and at least up to ~200 km offshore (e.g. Muñoz et al., 2011; Zheng et al., 2011; their Fig. 6) the regional zonal circulation results in enhanced flow divergence (i.e. subsidence) in the afternoon over the coast and convergence at dawn, partially explaining the tendency for clear/overcast skies in the afternoon/morning. Although the austral winter-spring synoptic-scale signal from mid-latitude weather disturbances is not very relevant when compared with diurnal cycles at these latitudes, observed day-to-day oscillations in the coastal MBL depth resulting from interactions of this synoptic-scale signal with the Andes and coastal mountain ranges, modify the MBL wind and cloudiness regimes (Rutllant et al., 1998, 2003), and must therefore be considered in this analysis. In particular, the effect of episodic strong easterly-wind events at about 2500 m altitude on the coastal Sc, occurring from four to eight times per year, were studied by Huneeus et al. (2006), based on the Antofagasta (Cerro Moreno Airport) radiosonde data. For a particular event, these authors compared results of a numerical simulation of the associated transport and deposition of sulfur aerosols from several copper-smelter emissions in the area, with anomalies in Sc cloud droplet number concentrations observed in the satellite imagery, resulting them qualitatively consistent. Synoptic conditions associated with these strong easterly wind events were found similar to those associated with the onset of coastal troughs/lows in Central Chile (Garreaud et al., 2002).

VOCALS-REx took place between 15 October and 14 November 2008, when observations from different platforms (on board from research vessels and airborne from different airplanes) were combined with surface-based observations along the coast of Northern Chile. A land-site was previously selected to perform in-cloud measurements

ACPD
12, 22783–22811, 2012

and surface meteorological observations. The selected place was Paposo Alto (PA) (∼25° S; 70.5° W) over a relatively flat surface at about 700 m a.m.s.l. in the southern portion of the VOCALS-REx study area. Radiosonde and additional surface meteorological observations were performed at Paposo Bajo (PB), a fishermen village at the foothill of PA.

This paper is aimed at characterizing mean diurnal cycles of the atmospheric circulation and at interpreting the day-to-day variability of the measured meteorological variables during VOCALS REx, both within and above the MBL up to ∼4000 m a.m.s.l., where the effect of the Andes is manifested. To further document the afternoon increase in coastal subsidence resulting from the mean diurnal cycles of the zonal wind above the MBL and, in particular, its offshore extension, a numerical simulation of the regional circulation with the Weather Research and Forecasting (WRF) model was performed for four consecutive days in October 2008, at 2 km resolution, when atmospheric conditions remained fairly stationary. The paper is organized as follows. After describing the ground site, the surface and upper-air meteorological data collected during the experiment and the model setup for the numerical simulation in Sect. 2, the main features of the diurnal cycles and their numerical simulation are presented in Sect. 3, followed by a characterization of the day-to-day variability in response to synoptic-scale weather conditions during VOCALS-REx. A summary and discussion are presented in Sect. 4.

2 Data and methods

Between 15 October and 14 November 2008, land-based meteorological observations were carried out at Paposo (∼25.1° S), in the southern part of the VOCALS-REx area (Fig. 1). Surface meteorological observations were averaged every 5 min through standard tripod-mounted Campbell automatic weather stations at Paposo Bajo (PB), near sea-shore, and at Paposo Alto (PA) located on a coastal flat just above PB at ∼700 m

ACPD
12, 22783–22811, 2012

a.m.s.l. (Table 1). Wind sensors were located at ~4 m from the ground on top of the tripod.

PA was selected as the land-site for "in-cloud" surface-based observations during VOCALS- REx. In fact, not only PA is located near the top of the MBL, but it is a place where Sc clouds tend to persist due to the coastline shape (i.e. embayment between Point Pasallaves (~24.8° S), north of Paposo, and Point San Pedro (~25.4° S), to the south), as depicted in a low-cloud climatology along the coast of North-Central Chile (Gonzalez et al., 2007) and manifested in a dense garden of native shrubs along the windward side of the coastal flat. There, experiments of cloud-water collection have been conducted in the past.

An important PA orographic feature of the coastal mountain range is the proximity of several "sierras" (e.g. Vicuña Mackenna, Amarilla, Peñafiel) as counterforts of the Andes cordillera, with elevations in excess of 2000 m within a few tens of km away from the coastline. These sierras favor either channeling of the prevailing northwesterly wind ("barrier flow") above the MBL, or enhanced blocking of the westerly (onshore) wind component advecting stable air within the subsidence inversion layer on to the coastal mountains.

Upper air observations consisted of Vaisala RS80-15G radiosonde launchings at PB (00:00 and 12:00 UTC: 17–23 October; 00:00, 12:00 and 21:00 UTC: 24 October–9 November; 00:00, 06:00, 18:00, 21:00 UTC: 11–12 November; 00:00, 06:00, 12:00, 18:00, 21:00 UTC: 13–15 November). Additional soundings were performed at Cerro Moreno (CM: Antofagasta airport: 00 and 12:00 UTC); and at Iquique (NCAR/EOL GAUS: 00:00, 04:00, 08:00, 12:00, 16:00, 20:00 UTC). Previous (24–29 January 1997) Michilla radiosoundings, at 00:00, 06:00, 12:00, 18:00 UTC, have been included here for reference. Figure 1 depicts the location of these upper-air observations along with three topographic W–E cross-sections spanning the study area. There, the coastal cliff and mountain ranges, with an average elevation exceeding 1000 m, confine the coastal MBL and associated Sc clouds on its top, to a narrow (~10 km wide) coastal-desert strip. The Andean western slope is particularly steep and uniform inland of Iquique. In order to gain more insight into space and time variability, complementary coastal observations included surface meteorological data at Caleta Constitución (CC: ~23.4° S), operative since 1997 with a few data gaps, and Michilla (~22.7° S) radiosonde observations in January 1997 during the DICLIMA Experiment (Rutllant et al., 1998, 2003).

To supplement the observational results we performed a short-term, high-resolution numerical simulation using the WRF model. The model was initialized at 18:00 UTC, 30 September 2008, and integrated continuously for the next four days. We chose this period within VOCALS-REx because it featured particularly stable synoptic conditions (e.g. Rahn and Garreaud, 2010b), so that average diurnal cycles are meaningful. Results presented here are taken from the inner domain with a horizontal grid spacing of 2-km and 44 σ-levels in the vertical with telescoping resolution toward the surface. The inner domain, spanning a rectangular region from 18–26° S and 77–66° W, was embedded in a larger domain. Parameters used for the run include the Thompson microphysics scheme, rapid radiative transfer model and Dudhia radiation schemes, Monin-Obukhov (Janjic) surface scheme, Pleim land-surface model, Mellor-Yamada-Janjic boundary layer scheme, Betts-Miller-Janjic cumulus scheme, second-order turbulence and mixing, and a horizontal Smagorinsky first-order closure eddy coefficient.

The authors are well aware of the deficiencies of WRF – as well as other numerical models – in simulating the MBL in the near-shore area. Indeed, several works have shown that the modeled MBL is substantially shallower (by a factor 2) than observed (e.g. Garreaud and Muñoz, 2005; Rahn and Garreaud, 2010a; Sun et al., 2010; Wyant et al., 2010), which hinders the model capability of simulating the coastal cloud deck. The problem is only slightly attenuated by increasing horizontal or vertical resolution. Nevertheless, here we focus on the regional-scale circulation in the free troposphere above the MBL, where, as we show later, the WRF simulation was able to resolve the diurnally varying, topographically forced wind system.

ACPD
12, 22783–22811, 2012

3 Results

3.1 Mean diurnal cycles

As mentioned before, diurnal cycles are by far more important than the synoptic-scale changes in late spring over the study area. Diurnal cycles of surface winds and marine boundary layer structure over the subtropical Southeast Pacific have been described and analyzed in Muñoz (2008) and in Rahn and Garreaud (2010a), respectively. Figure 2 represents diurnal mean cycles of vertical wind profiles and air temperature for the upper-air measuring sites during VOCALS-REx (i.e. Paposo and Iquique), together with those from Michilla for January 1997 during neutral ENSO conditions.

Above the MBL, and except for minor differences between them, an inland flow ($U > 0$) is observed at around 1000–2500 m, peaking at ∼1700 m altitude centered at 18:00 LT (UTC−4) at Iquique and Michilla, but at ∼14:00 LT at Paposo. Reasons for this phase shift in the timing of the maximum diurnal upslope flow are not yet clear. A weaker seaward return flow appears around 3000 m altitude. The nocturnal phase of this cycle, much less intense than the daytime one, is observed at about the same altitude range, peaking around 08:00 LT. These results are generally consistent with those from previous studies (Rutllant et al., 2003). At Paposo the separation of the breeze systems below and above 1000 m is especially clear. Below 1000 m (i.e. within the MBL) the afternoon westerly wind component prevails from 0 to 500 m while the easterly one appears between 500 and 1000 m. The nocturnal phase is much weaker.

The mean meridional wind component (V) shows invariably northerlies above the MBL, in particular for Iquique and Paposo during VOCALS-REx, as also observed at Point Alpha at about 200 km off Iquique (Zheng et al., 2011; their Fig. 6). The ubiquitous northerly wind components at altitudes below the mean top of the Andes is presumably related to the blocking of the westerly flow components under thermodynamically stable conditions (i.e. small Froude numbers), with the subsequent formation of a barrier jet, as documented for Central Chile (Rutllant and Garreaud, 2004). To emphasize this feature and, in particular, its manifestation at different heights below the Andes

Discussion Paper | Discussion Paper | Discussion Paper | Discussion Paper |
ACPD
12, 22783–22811, 2012

top, Fig. 3 illustrates the mean frequency distribution of wind directions at Antofagasta (Cerro Moreno Airport) as a function of standard heights up to 6000 m a.s.l. at (a) 12:00 UTC (08:00 LT) and (b) 00:00 UTC (20:00 LT) for the period when both observing hours were available (1961–1987, see Muñoz et al., 2011). Northerlies prevail above the MBL, at least up to 3000 m altitude, shifting gradually to westerlies above the Andes with increasing frequency up to the tropopause (not shown). At 12:00/00:00 UTC these northerlies stay within the NE/NW quadrant at Fig. 3a, b. During austral summer (November to March: not shown) near-surface southerlies and NNEs centered at 2000 m are more persistent; the shape of the distribution remaining almost invariable throughout the year.

Within the MBL, Fig. 2 shows that southerly (S–SW) components peak between 16:00 and 18:00 LT, alternating with northerly (NE) ones at dawn at Iquique and partially at Michilla. The fact that at Paposo southerlies (SW) apparently prevail throughout the day is probably due to the lack of nocturnal launchings. Continuous surface observations at PB and PA (Fig. 4) show nighttime and early morning surface winds from the NE quadrant (see Fig. 4e), as observed at Iquique. In general, southerly wind components peak at about 18:00 LT, when clear skies prevail along the coastal strip (e.g. Muñoz et al., 2011). Additional time series and mean diurnal cycles of surface-based observation of air temperature, downwelling solar radiation, net radiation, relative humidity/mixing ratio and atmospheric pressure at PA and PB during VOCALS-REx are included as Supplement in Annex 1.

3.2 Afternoon increase in coastal subsidence

The DICLIMA experiment (Rutllant et al., 2003) provided evidence to test the hypothesis of an increase in subsidence in the late afternoon (Rutllant and Ulriksen, 1979) along the coast due to the boundary layer divergence of the daytime upslope flow above the subsidence inversion, centered at about 2000 m altitude. This extra subsidence, ultimately related to the daytime solar heating of the western slope of the Andes, could explain the descent of the subsidence inversion base in the late after-

ACPD
12, 22783–22811, 2012

noon (Rutllant et al., 2003) and a small temperature increase at the inversion top. The importance of the diurnal cycle of vertical velocity coupled with the thermal structure just above the subsidence inversion was addressed through a numerical model simulation by Muñoz (2008). There, coastal subsidence at ~24–26° S maximizes between 2000–3000 m altitude with peak values al local noon, extending through the afternoon (Muñoz, 2008; his Fig. 12). Associated temperature tendency due to vertical advection amounted to 0.75 $\mathrm{K\,h^{-1}}$ producing maximum warming at about 15:00 LT (Muñoz, 2008; his Fig. 11). This warming is replicated in Fig. 2 at Paposo at 20:00 LT (00:00 UTC), and earlier at Iquique and Michilla. Furthermore, the time series of potential temperature with height at Paposo (Fig. 5a) consistently shows minimum inversion bases at 00:00 UTC, in particular during the period of large amplitude diurnal cycles (i.e. 4–9 November).

Additional evidence of this late afternoon warming can be seen in Fig. S1, in which maximum temperatures at PA lag those at PB by about two hours, with a corresponding signal existing in relative humidity (Fig. S3). Moreover, this coastal afternoon extra subsidence should be connected with the observed depression of the MBL (Fig. 5a), possibly contributing to the tendency of coastal Sc to clear in the afternoon, as depicted in Fig. 6 in which PM-AM Sc cloud cover from GOES images evidences a climatological afternoon clear strip of about 50 km. Around dawn, cooling at about the subsidence inversion base, noticeable at Paposo and Michilla, could be associated either to the radiative cooling at the top of the Sc cloud deck or to the "upsidence wave" described in Garreaud and Muñoz (2004).

3.3 Numerical simulation of wind and temperature daily mea cycles

To assess the offshore extent of this extra subsidence in the afternoon, Fig. 7 represents a U and W cross section averaged over 19–22° S, centered at ~70° W for 07:00 LT and 17:00 LT (average of the 4-day WRF run), representing the extremes of the diurnal cycle. Recall that we focus here on the regional circulation above the MBL. At dawn there is a weak (less than 1 $\mathrm{m\,s^{-1}}$) downslope flow with a hint of convergence

ACPD
12, 22783–22811, 2012

above the coastline. The pattern changes dramatically during afternoon so that by 17:00 LT there is a strong (> 5 $m s^{-1}$) upslope flow from the coastal mountains inland, leading to marked divergence over the coastal area. This diurnally varying regional pattern is in good agreement with the DICLIMA observations (Rutllant et al., 1998, their Fig. 8). The most relevant changes in vertical velocity occur between 800–850 hPa and are depicted by the daily march of W at 820 hPa. Figure 8, zooming in the coastal area, illustrates the onset of the subsidence increase at about 15:00 UTC (11:00 LT) peaking between 18:00 and 21:00 UTC (14:00 and 17:00 LT) in a narrow band less than 10 km wide. To further characterize the timing of the maximum coastal subsidence and associated warming, mean hourly vertical profiles at P (see Fig. 7) of W and temperature anomalies relative to the corresponding hourly averages (T') shown in Fig. 9 illustrate the afternoon increase in subsidence centered at ~820 hPa concomitant with maximum positive T' values (~1 °C). At about 960 hPa, positive vertical velocities peak around 16:00 UTC (12:00 LT) with negative temperature anomalies. Here it is important to note again that near the coast the WRF model fails in reproducing a realistic MBL and the associated cloud deck at its top (e.g. Zeng et al., 2004; Garreaud and Muñoz, 2005).

3.4 Synoptic-scale variability

Alongshore-oriented coastal and inland mountain ranges, in combination with a quasi-permanent subsidence inversion frequently below the mean coastal mountains altitude within the study area, can sustain poleward-propagating wave-like phenomena whose pace is at least partially synchronized with synoptic-scale mid-latitude, eastward-travelling troughs and ridges in the upper troposphere. Thus, amplitude and timing of diurnal cycles, including the depth of the marine boundary layer, are regularly modulated by sub-synoptic to synoptic-scale disturbances, the latter described and analyzed for the whole VOCALS-REx area in Rahn and Garreaud (2010b) (hereinafter referred to as RG).

ACPD
12, 22783–22811, 2012

Day-to-day changes in the depth of the well-mixed MBL, represented as the height of the base of the subsidence inversion layer in a time-height cross section of potential temperature at PB (Fig. 5a), exhibit up and down excursions from a mean depth of ∼1000 m. In several occasions during the experiment, PA (dashed line) was immersed in the warm-dry air on top of the clouds. As mentioned before, particularly regular diurnal cycles can be observed from 4 to 9 November with minimum depths late in the afternoon (∼20:00 LT), the lowest depth being reached on the 6th. Above the MBL, this sequence is mimicked by strong north-westerlies (Fig. 5b, c). This period also features high diurnal ranges in near-surface air temperature and relative humidity at both PB and PA, under mostly clear skies (Figs. S1–S3).

In the synoptic scale, the MBL top sharply raised on 24 October and more gradually towards the end of the field experiment (November 14–15). In the former case, enhanced northwesterly winds in the free troposphere and a dip in the 500 hPa geopotential heights indicated mid-troposphere troughing (T3 in RG). The latter conditions occurred under the influence of a cutoff low (see RG). In fact, from 11–14 November SSE winds in the middle troposphere sharply veered to NNW on 14–15 November (Fig. 5b, c). Concomitant with this wind reversal, ridging and warming of the middle troposphere since 6 November gave way to a sudden cooling on the 14.

Minimum MBL depths, with the subsidence inversion base marginally touching PA, occurred on 30 October and on 3 and 6 November, with light NE winds and pressure minima recorded at PB (Fig. S4). Simultaneous time series of 500 and 1000 hPa geopotential heights (RG) show ridging at 500 hPa and a simultaneous drop in 1000 hPa heights, resulting into high 1000–500 hPa thicknesses, indicating easterly warm advection in the lower troposphere, as described for Central Chile in Garreaud el al. (2002), Garreaud and Rutllant (2003), Rutllant and Garreaud (2004); and for the Antofagasta region in Rutllant et al. (1998, 2003). Such conditions occurred on 26 October, 2 and 11 November. Low MBL depths in-between probably correspond to sub-synoptic, wave-like oscillations without any apparent mid-latitude connection (Fig. 5a). These local/regional oscillations (2 to 4-day period) in the MBL depth can be

Discussion Paper | Discussion Paper | Discussion Paper | Discussion Paper |

ACPD

12, 22783–22811, 2012

Meteorological observations during VOCALS-REx

J. A. Rutllant et al.

better identified in the radiosonde data from Iquique, about 500 km north of Paposo (not shown).

Near-surface maximum wind speeds around 6 m s^{-1} in the afternoon at PB occurred on 13–14 October, 20 October, 27–29 October, and 6–8 November (Fig. 4a) coincident with those at Caleta Constitución (CC: 23.4° S, not shown), although the latter surpassed by ~50 % those at PB. The synoptic-scale modulation (i.e ~7-day periods) in these maximum afternoon wind speeds featured, near the end of these periods, minima in atmospheric pressure (Fig. S4) on 21–22 October, 29 October, and 6 November, accompanied by enhanced NE winds at early morning, also coinciding in general with minima in the MBL depth. This co-variability between atmospheric pressure and MBL depth minima immediately following afternoon wind maxima is again very similar to that characterizing coastal lows in Central Chile (op. cit.), and coincide with the onset of ridging in the mid-troposphere. Similar conditions have been reported from the Antofagasta radiosonde data by Huneeus et al. (2006) for strong easterly wind events at 700 hPa and by Velásquez (2010) while climatologically characterizing the synoptic patterns associated to the extremes in the MBL depth variability.

Deeper downward excursions of the base of the subsidence inversion leaving PA just above the MBL in late austral winter and early spring previous to VOCALS-REx, occurred in 5 occasions in which strong morning NE winds (~10 m s^{-1}) interrupted for a few hours the otherwise light-wind conditions (~1 to 2 m s^{-1}) prevailing there, with jumps of around 10 °C in temperature, relative humidity drops down to 10 % and minimum SLPs. Though regional surface and upper-air features (not shown) during these events are consistent with mid-latitude synoptic-scale forcing of coastal lows (e.g. Garreaud et al., 2002; Huneeus et al., 2006), their impact on the local Sc cloud cover is negligible since Paposo is located within an area of high Sc persistence (González et al., 2007). As expected, in late spring during VOCALS-REx, the mean MBL depth is higher than in early spring, while mid-latitude synoptic-scale forcing gradually fades away. This results in weaker and fewer episodes in which the subsidence inversion descends below PA.

Discussion Paper | Discussion Paper | Discussion Paper | Discussion Paper |

ACPD
12, 22783–22811, 2012
Meteorological observations during VOCALS-REx
J. A. Rutllant et al.

Title Page
Abstract Introduction
Conclusions References
Tables Figures
◀◀ ▶▶
◀ ▶
Back Close
Full Screen / Esc
Printer-friendly Version
Interactive Discussion

4 Summary and discussion

Land-based surface and upper air meteorological observations during VOCALS-REx are analyzed in this short, mostly descriptive, contribution under the assumption that mean diurnal circulation cycles within and above the marine boundary layer (MBL, with a mean depth of ∼1000 m) can significantly contribute to the aerosol transport from near shore and inland emissions to the offshore cloud-topped MBL in austral spring, when the study area features maximum cloud cover and intensity of the SE Pacific subtropical anticyclone. Surface observations included automatic weather stations at Paposo Alto (PA, ∼700 m a.s.l) and Paposo Bajo (PB: sea level). Radiosonde observations were carried out at PB and Iquique. Michilla radiosonde data for January 1997 (austral summer) have been included as well for comparison.

Within the MBL, the mean nocturnal (i.e. AM) flow shows weak near-surface northeasterlies shifting gradually to southeasterlies at early morning, with a return northwesterly flow aloft (Iquique and Michilla). This period is not well represented at Paposo where, for most of the time, no soundings were performed out of the 08:00–20:00 LT period. This pattern clearly reverses in the afternoon (PM), when strong near-surface southwesterlies gradually decrease in strength with height, reaching minimum speeds near the MBL top (i.e ∼1000 m). At Paposo these afternoon MBL winds actually turn into southeasterlies near the MBL top. In summary, within the coastal MBL, characteristic sea-land breezes are superimposed on the prevailing southerlies, resulting in light northeasterly winds from mid-night to early morning and strong near-surface southwesterlies in the afternoon, with their corresponding return flows near the MBL top.

Above the MBL a strong inland WSW afternoon flow between 1500 m and 2000 m peaks at around 1700 m in the northern part of the study area (i.e. Iquique) contrasting with NW winds over Paposo at those heights, peaking at around the time of maximum solar warming over the Andes western slope. The seaward return flow is from the NNE, peaking in the late afternoon at about 3000 m altitude at Iquique. At nighttime and early morning NNE winds replace the daytime WSW ones at ∼1000–2500 m altitude, with an

ACPD
12, 22783–22811, 2012

Meteorological observations during VOCALS-REx

J. A. Rutllant et al.

inland return flow from the NNW at 2000–4000 m altitude. The seaward return flow from the daytime, near-surface upslope flow could be eventually enhanced during austral summer by easterlies above the Andes (e.g. Garreaud, 2009), as seen in the Michilla mean diurnal cycles in January 1997 (Fig. 2).

In summary, the prevailing flow from the N above the MBL and below the Andes top (Fig. 3) is modulated by the onshore–offshore (zonal) flow components of the regional circulation induced by the diurnal cycle of the radiative heating/cooling along the western slope of the Andes. Altogether, the diurnal cycle of the zonal component of this regional circulation is consistent with an enhanced coastal subsidence in the afternoon that results in a lower subsidence inversion base and a slight warming at the inversion top. A numerical simulation of the zonal atmospheric circulation in a regional domain from the ocean to the Andes (19–22° S) captures the afternoon mean zonal wind divergence and the resulting subsidence along a narrow (∼10 km) coastal strip peaking at around 16:00 LT, partially explaining the afternoon Sc clearing tendency observed in GOES imagery, as evidenced in Fig. 6.

Day-to-day variability during VOCALS-REx shows 2 to 4-day oscillations in the MBL depth, aside from two major disruptions on 24 October in connection with a deep trough and a cutoff low on 14–15 November, as described in Rahn and Garreaud (2010b). These oscillations in the MBL are closely tied in phase to sea-level pressure and to the strength of the alongshore MBL southerlies in the afternoon, as found in coastal low-like propagation farther south (e.g. Garreaud et al., 2002), ultimately in response to the interaction of mid-latitude synoptic-scale disturbances and major alongshore orography.

Due to particular coastal topographic features north of Paposo, exceeding 2000 m altitude, either wind channeling or blocking of the onshore flow component of the northwesterlies above the MBL against the topography under enhanced afternoon subsidence along the coastal strip could at least partially explain those strong NW winds above the MBL, including strong northerly wind events recorded al PA in early spring previous to VOCALS-REx.

ACPD
12, 22783–22811, 2012

Title Page
Abstract Introduction
Conclusions References
Tables Figures
◀ ▶
Back Close
Full Screen / Esc
Printer-friendly Version
Interactive Discussion

Beyond a preliminary study of strong easterly wind episodes in Northern Chile (Huneeus et al., 2006), a simple scale analysis of trajectories with the data obtained here indicates that the mean afternoon seaward transport of sulfur dioxide from an inland (∼150 km), elevated source (∼2800 m altitude large copper smelter), with a typical speed of 5 m s^{-1} (as observed at Iquique at around 20:00 LT), would take about 10 h to reach the coast (dawn next day) at a time of maximum coastal eastward flow just above the subsidence inversion. Therefore, it is likely that those westward trajectories would be re-directed inland before actually reaching the cloud top. The typical speed of the daytime return flow is consistent with those observed at Baquedano and Michilla in January 1997 during the DICLIMA Experiment (Rutllant et al., 2003).

From this analysis one could tentatively conclude that the mean seaward transport of sulfur dioxide from inner, elevated sources (>∼ 2500 m altitude), could be related to the general seaward flow component at those heights that peak late in the afternoon, embedded in a mean northerly flow, with a delay of the order of at least one day. Within the MBL, biogenic dimethylsulfide (DMS) could be more easily degassed in the afternoon due to the strengthening of the SW winds, while other inland coastal sources could contribute preferentially at dawn, coinciding with the maximum coastal low-cloud cover.

The capacity of the daytime mean return flow, within and above the MBL, to transport oxidized sulfur emissions seaward, should be studied in detail using transport and dispersion models tailored for the complex orography of this region.

Supplementary material related to this article is available online at: http://www.atmos-chem-phys-discuss.net/12/22783/2012/acpd-12-22783-2012-supplement.pdf.

Acknowledgements. We want to thank here all the participants in the field work at Paposo, including personnel from the Chilean Weather Service (DMC) who took care of the radiosonde launchings at PB. Radiosondes were kindly provided by Bruce Albrecht. Special thanks are

ACPD
12, 22783–22811, 2012

also due to Ana Maria Cordova for general coordination at the Paposo site. We are also grateful for the facilities granted by the Paposo school and by the National Forestry Corporation (CONAF) at PA. Alejandra Molina kindly compiled the reflectivity fields used in the construction of Fig. 9. Support for the meteorological field work at Paposo was provided by the Department of Geophysics, Universidad de Chile. The NCAR Earth Observatory Laboratory provided field logistics and data archival of Iquique radiosoundings.

References

Bretherton, C. S., Uttal, T., Fairall, C. W., Yuter, S. E., Weller R. A., Baumgardner, D., Comstock, K., Wood, R., and Raga, G. B.: The EPIC 2001 stratocumulus study, B. Am. Meteorol. Soc., 85, 967–977, 2004.

Garreaud, R. D.: The Andes climate and weather, Adv. Geosci., 22, 3–11, doi:10.5194/adgeo-22-3-2009, 2009.

Garreaud, R. and Muñoz, R.: The diurnal cycle of circulation and cloudiness over the subtropical Southeast Pacific: a modeling study, J. Climate, 17, 1699–1710, 2004.

Garreaud, R. and Muñoz, R.: The low-level jet off the west coast of subtropical South America: structure and variability, Mon. Weather Rev., 133, 2246–2261, 2005.

Garreaud R. and Rutllant, J.: Coastal Lows along the subtropical west coast of South America: numerical simulation of a typical case, Mon. Weather Rev., 131, 891–908, 2003.

Garreaud R., Rutllant, J., and Fuenzalida. H.: Coastal lows along the subtropical west coast of South America: mean structure and evolution, Mon. Weather Rev., 130, 75–88, 2002.

González C., Rutllant, J., and Paolini, P.: Frecuencia y Albedo de Estratocúmulos Costeros entre 24–32° S, Cuarto Taller Circulación Océanica y Atmosférica en el Pacífico SE (DOCA), Dirección Meteorológica de Chile, Santiago, Chile, 18–19 October, 2007.

Huneeus, N., Gallardo, L., and Rutllant, J.: Offshore transport episodes of anthropogenic sulfur in Northern Chile: potential impact on the stratocumulus cloud deck, Geophys. Res. Lett., 33, L19819, doi:10.1029/2006GL026921, 2006.

Muñoz, R.: Diurnal cycle of surface winds over the subtropical Southeast Pacific, J. Geophys. Res., 113, D13107, doi:10.1029/2008JD009957, 2008.

Muñoz R., Zamora, R., and Rutllant, J.: The coastal boundary layer at the eastern margin of the South East Pacific (23.4° S, 70.4° W): cloudiness conditioned climatology, J. Climate, 24, 1013–1033, 2011.

Painemal, D., Garreaud, R., Rutllant, J., and Zuidema, P.: Southeast Pacific stratocumulus: high frequency variability and meso-scale structures over San Félix Island, J. Appl. Meteorol. Clim., 49, 463–477, 2010.

Rahn, D. A. and Garreaud, R.: Marine boundary layer over the subtropical southeast Pacific during VOCALS-REx – Part 1: Mean structure and diurnal cycle, Atmos. Chem. Phys., 10, 4491–4506, doi:10.5194/acp-10-4491-2010, 2010a.

Rahn, D. A. and Garreaud, R.: Marine boundary layer over the subtropical southeast Pacific during VOCALS-REx – Part 2: Synoptic variability, Atmos. Chem. Phys., 10, 4507–4519, doi:10.5194/acp-10-4507-2010, 2010b.

Rutllant J. and Garreaud, R.: Episodes of strong flow down the western slope of the subtropical Andes, Mon. Weather Rev., 132, 611–622, 2004.

Rutllant J. and Ulriksen, P.: Boundary-layer dynamics of the extremely arid northern part of Chile: the Antofagasta field experiment, Bound-Lay. Meteorol., 17, 41–55, 1979.

Rutllant J., Fuenzalida, H., Torres, R., and Figueroa, D.: Interacción océano atmósfera tierra en la región de Antofagasta (Chile, 22° S): experimento DICLIMA, Rev. Chil. Hist. Nat., 71, 405–427, 1998.

Rutllant J., Fuenzalida, H., and Aceituno, P.: Climate dynamics along the arid northern coast of Chile: the 1997–1998 Dinámica del Clima de la Región de Antofagasta (DICLIMA) experiment, J. Geophys. Res.-Atmos., 108, D174358, doi:10.1029/2002JD003357, 2003.

Spak, S. N., Mena, M., and Carmichael, G.: Atmospheric transport of anthropogenic oxidized sulphur over the Southeast Pacific during VOCALS REx, CLIVAR Exchanges, 15, 20–21, 2010.

Sun, R., Moorthi, S., Xiao, H., and Mechoso, C. R.: Simulation of low clouds in the Southeast Pacific by the NCEP GFS: sensitivity to vertical mixing, Atmos. Chem. Phys., 10, 12261–12272, doi:10.5194/acp-10-12261-2010, 2010.

Velásquez, P. A.: Patrones sinópticos asociados a la variabilidad de la capa límite marina en Antofagasta, Chile, Undergraduate thesis, Universidad de Valparaíso, Chile, 2010.

Wood, R., Mechoso, C. R., Bretherton, C. S., Weller, R. A., Huebert, B., Straneo, F., Albrecht, B. A., Coe, H., Allen, G., Vaughan, G., Daum, P., Fairall, C., Chand, D., Gallardo Klenner, L., Garreaud, R., Grados, C., Covert, D. S., Bates, T. S., Krejci, R., Russell, L. M.,

ACPD
12, 22783–22811, 2012

Meteorological observations during VOCALS-REx

J. A. Rutllant et al.

de Szoeke, S., Brewer, A., Yuter, S. E., Springston, S. R., Chaigneau, A., Toniazzo, T., Minnis, P., Palikonda, R., Abel, S. J., Brown, W. O. J., Williams, S., Fochesatto, J., Brioude, J., and Bower, K. N.: The VAMOS Ocean-Cloud-Atmosphere-Land Study Regional Experiment (VOCALS-REx): goals, platforms, and field operations, Atmos. Chem. Phys., 11, 627–654, doi:10.5194/acp-11-627-2011, 2011.

Wyant, M. C., Wood, R., Bretherton, C. S., Mechoso, C. R., Bacmeister, J., Balmaseda, M. A., Barrett, B., Codron, F., Earnshaw, P., Fast, J., Hannay, C., Kaiser, J. W., Kitagawa, H., Klein, S. A., Köhler, M., Manganello, J., Pan, H.-L., Sun, F., Wang, S., and Wang, Y.: The PreVOCA experiment: modeling the lower troposphere in the Southeast Pacific, Atmos. Chem. Phys., 10, 4757–4774, doi:10.5194/acp-10-4757-2010, 2010.

Zeng, X., Brunke, M., Zhou, M., Fairall, C., Bond, N., and Lenshow, D.: Marine atmospheric boundary layer height over the Eastern Pacific: data analysis and model evaluation, J. Climate, 17, 4159–4170, 2004.

Zheng, X., Albrecht, B., Jonsson, H. H., Khelif, D., Feingold, G., Minnis, P., Ayers, K., Chuang, P., Donaher, S., Rossiter, D., Ghate, V., Ruiz-Plancarte, J., and Sun-Mack, S.: Observations of the boundary layer, cloud, and aerosol variability in the southeast Pacific near-coastal marine stratocumulus during VOCALS-REx, Atmos. Chem. Phys., 11, 9943–9959, doi:10.5194/acp-11-9943-2011, 2011.

ACPD
12, 22783–22811, 2012

Meteorological observations during VOCALS-REx

J. A. Rutllant et al.

Table 1. Sensors and equipment for PA and PB Campbell Scientific Inc. automatic weather stations, including installed/retired dates.

Name/Make	Model @PA	Model @PB
Pyranometer Apogee	PYR-P	PYR-P
Net radiometer Kipp & Zonen	NR Lite	NR Lite
Barometer Vaisala	PTB 101B	PTB 101B
Anemometer RM Young	03001 Wind Sentry	03001 Wind Sentry
T/HR Vaisala	HMP 45C	HMP 45AC
Data logger CSI	CR10X-2 Mega	CR10X
Installed/Retired	2008, 23 Jul/15 Nov	2008, 13 Oct/16 Nov

ACPD
12, 22783–22811, 2012

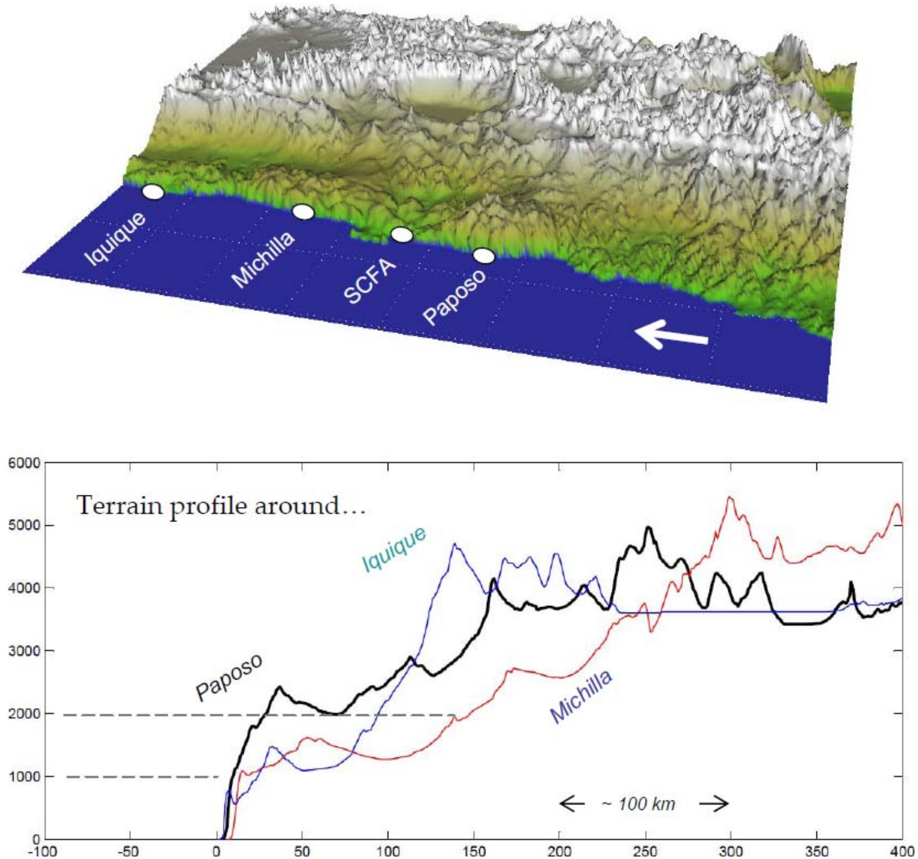

Fig. 1. Location of radiosonde observations referred to in the text (top panel) and topographic zonal (cross shore) cross-sections at the indicated sites (bottom panel).

ACPD

12, 22783–22811, 2012

Meteorological observations during VOCALS-REx

J. A. Rutllant et al.

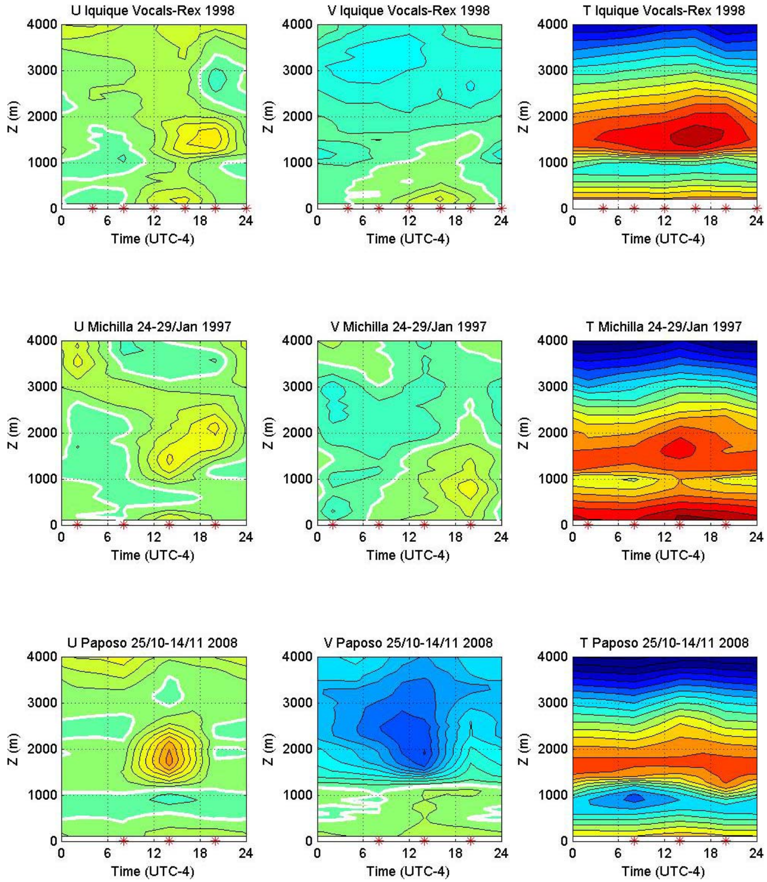

Fig. 2. Mean diurnal cycles from radiosonde data at Iquique and Paposo during VOCALS-REx, and from Michilla radiosondes in January 1997. Left panels: zonal wind component ($1\,\mathrm{m\,s^{-1}}$ contours; white contour is $0\,\mathrm{m\,s^{-1}}$). Center panels: id. for the meridional wind component. Right panels: air temperature (1 °C contours). Red stars in the time axis represent observing hours.

ACPD
12, 22783–22811, 2012

Meteorological observations during VOCALS-REx

J. A. Rutllant et al.

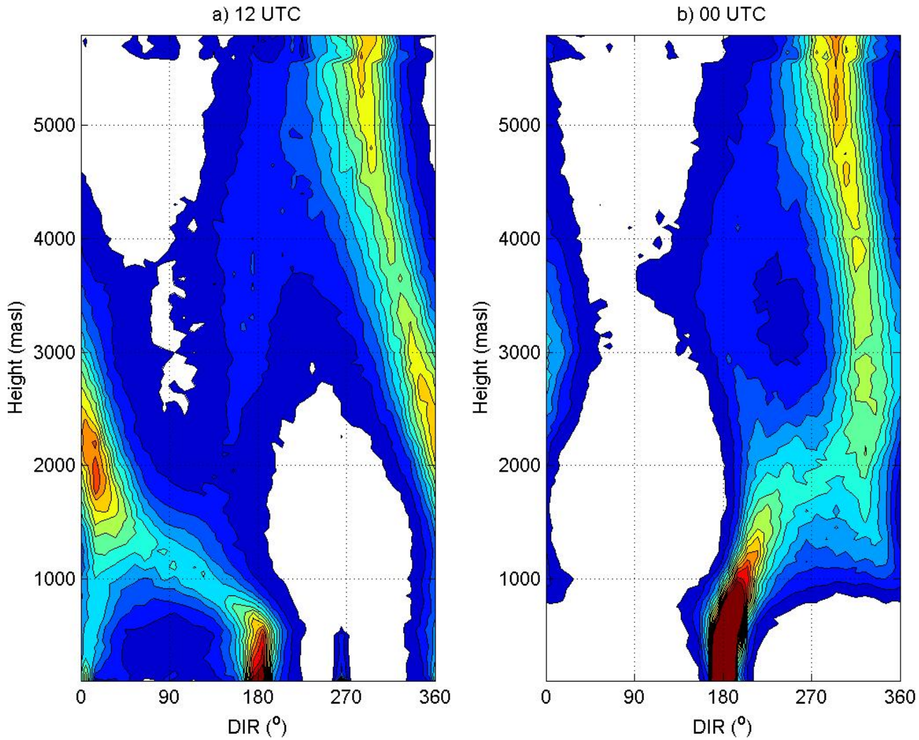

Fig. 3. Mean frequency distribution of wind directions at Antofagasta (Cerro Moreno Airport) at **(a)** 12:00 UTC (08:00 LT) and **(b)** 00:00 UTC (20:00 LT) as a function of standard height. A total of 5707 days in the 1961–1987 period was considered in the analysis for which 2-daily upper-air observations were available.

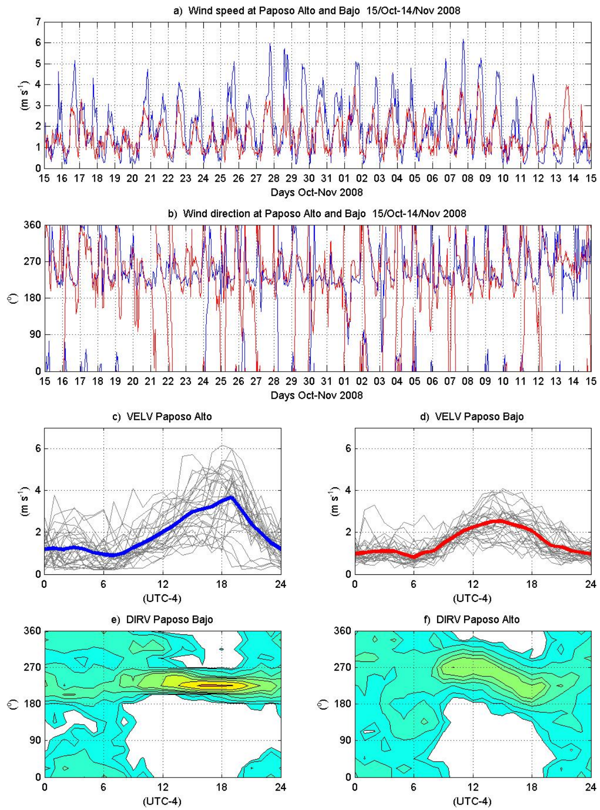

Fig. 4. (a) Time series of wind speed (hourly averages) measured at PA (blue) and PB (red); **(b)** as **(a)** but for wind direction, **(c)** diurnal cycle of wind speed at PA. Thin gray lines show daily series, the mean diurnal cycle in bold; **(d)** as **(c)** but for PB; **(e)** frequency of occurrence of wind directions throughout the day for PB, warmer colors depict higher frequencies; **(f)** as **(e)** but for PA.

ACPD
12, 22783–22811, 2012

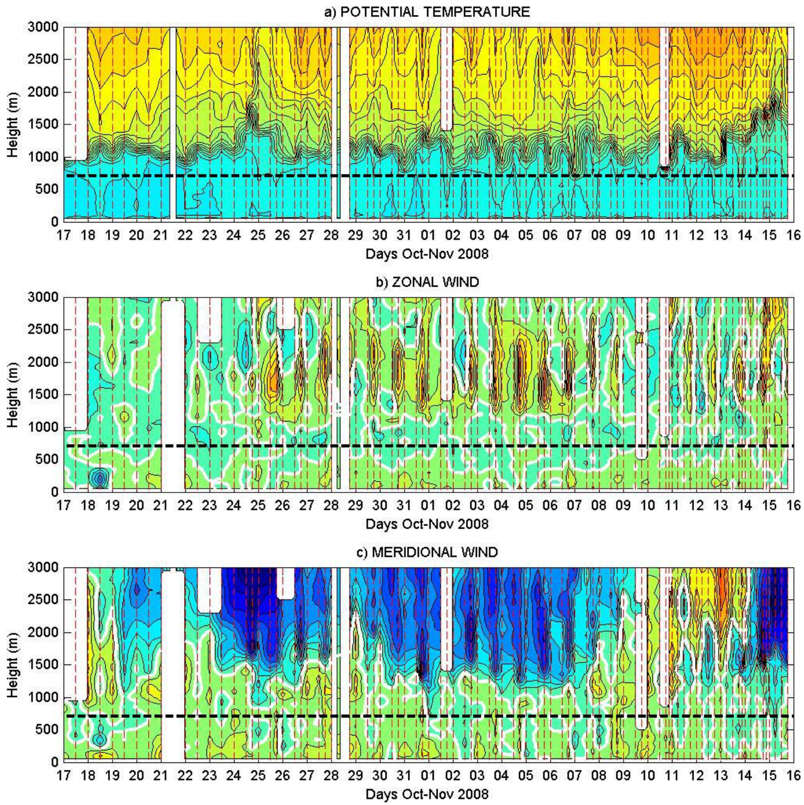

Fig. 5. Time-height cross sections of Paposo radiosonde observations during VOCAL-REx. **(a)** Potential temperature (contours every 2 K), **(b)** zonal wind component (contours every $2\,m\,s^{-1}$; white contour is $0\,m\,s^{-1}$), **(c)** as **(b)** but for the meridional wind component. Horizontal black dashed lines mark the altitude of PA. Vertical red dashed lines mark times of available radiosonde launchings.

ACPD
12, 22783–22811, 2012

Meteorological observations during VOCALS-REx

J. A. Rutllant et al.

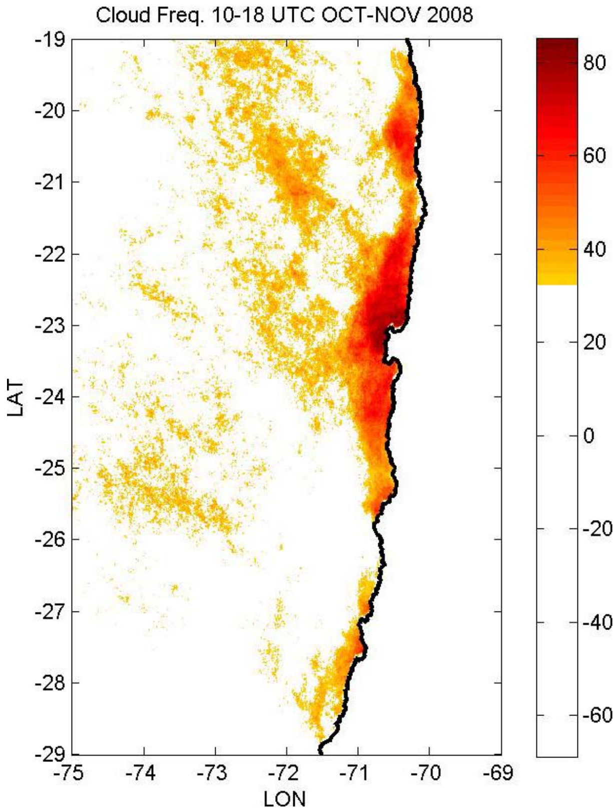

Fig. 6. Early morning (10:00 UTC) minus early afternoon (18:00 UTC) cloud frequency diagnosed from GOES visible imagery analysis for October/November 2008 period. A reflectivity threshold of 0.04 (0.10) was used to distinguish between cloudy and clear pixels in the visible image closest to 10:00 UTC (18:00 UTC). Cloud frequency drops below 30 % and over the continent have been masked out.

ACPD
12, 22783–22811, 2012

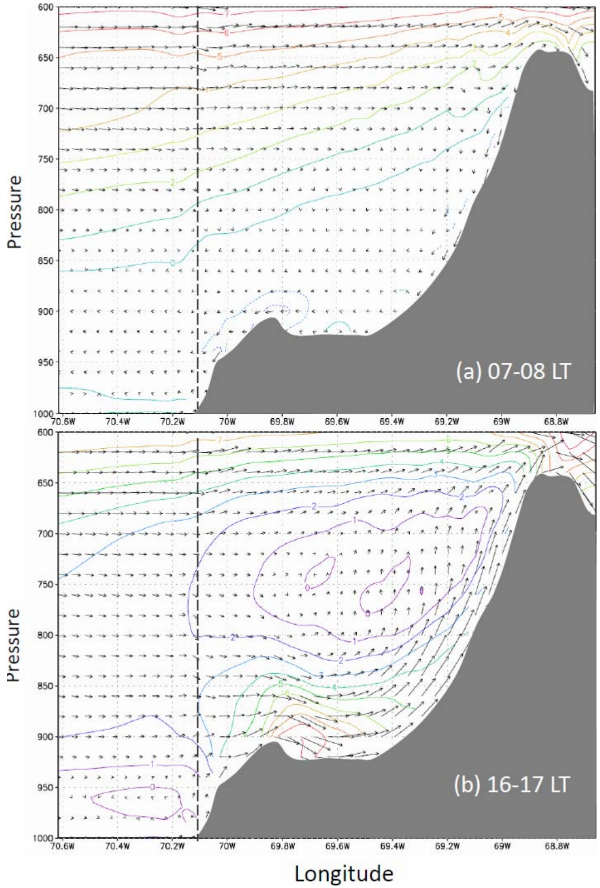

Fig. 7. WRF-simulated mean zonal (U) – vertical (W) wind vectors (arrows) in an average cross section between 19–22° S. Contours are zonal wind speeds: positive (solid) and negative (dashed) for **(a)** 07:00 LT, **(b)** 17:00 LT. The vertical dashed line represents the selected longitude for vertical profiles (P, see Fig. 9).

ACPD
12, 22783–22811, 2012

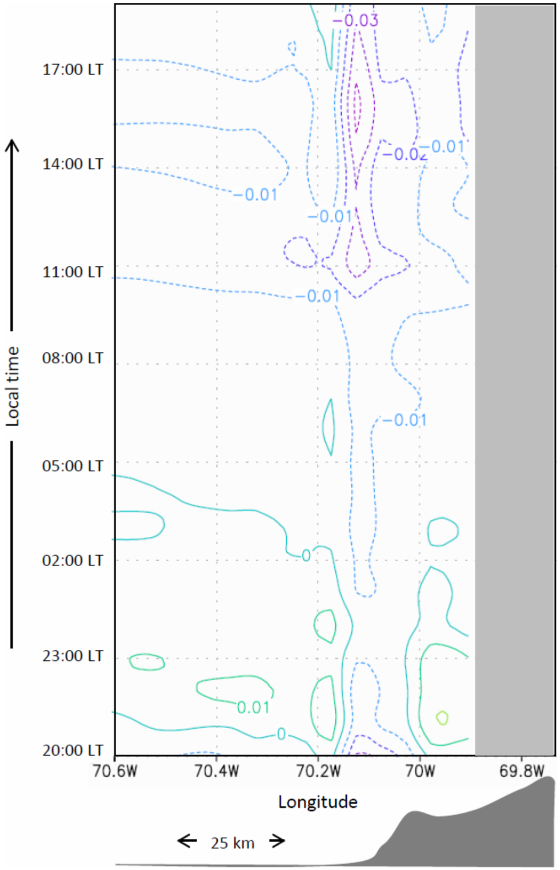

Fig. 8. Time – longitude cross section of the WRF-simulated vertical velocity (W, cm s^{-1}) at 820 hPa averaged between 19–22° S and over the 4-day run. Positive values (upward motion) in solid contour; negative ones (subsidence) dashed. The dark gray area at the bottom represents the average topographic profile. The light gray area to the right is where terrain elevation is above 820 hPa level.

ACPD
12, 22783–22811, 2012

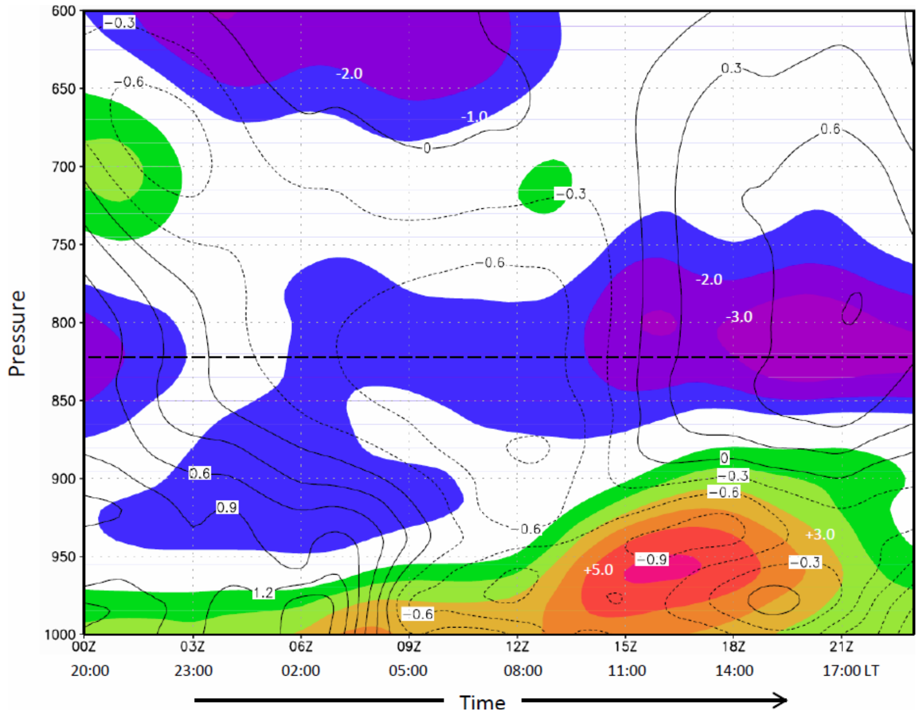

Fig. 9. Diurnal cycle of the vertical velocity (colors, in $cm\,s^{-1}$) and air temperature anomalies (contours: positive solid, negative dashed) with pressure at profile *P* (see Fig. 7) averaged between 19–22° S and over the 4-day run. Cold colors indicate subsidence, warm colors indicate ascent.

ACPD
12, 22783–22811, 2012